A simulation of liquid Cu and a comparison of sputtering of solid and liquid Cu under 1 keV

Ar$^+$ bombardment

A simulation of liquid Cu and a comparison of sputtering of solid and liquid Cu under 1 keV Ar$^+$ bombardment

Don E Harrison Jr†, Raol de Jesus Rodriguez and Roger Smith‡

Department of Physics, Naval Postgraduate School, Monterey, CA 93943, USA

Abstract. Techniques of simulating liquid Cu for the purpose of generating a target for a molecular dynamics simulation of the sputtering of liquid Cu have been investigated. The targets were generated by warming a solid Cu crystal in two different ways, first by assigning thermal velocities to the Cu atoms and secondly by thermal displacements increasing the target temperature in a series of warm cycles. The targets were then allowed to relax until equilibration occured. Targets with and without solid reflecting boundaries were examined and the resulting simulated liquid targets were compared. The target with the best liquid properties was then used for the sputtering simulation. The targets generated by these methods showed excellent agreement with both the Maxwell–Boltzmann distribution and the radial distribution function as measured by neutron diffraction. The preliminary sputtering investigation resulted in a sputtering yield increase of about 40% compared to that calculated for a low-index crystal plane.

1. Introduction

The sputtering of liquid surfaces by energetic ions has a number of potential applications. One such example applies to alloys where the high diffusion rate of the liquid state means that changes in surface composition due to preferential sputtering can be minimised. A second example occurs using a new technique for ion beam machining which involves the use of an ion source in very close proximity to an initially solid target. The high current densities and Ohmic heating of the target means that the surface layers become molten during the bombardment process.

There have been a number of experimental studies of the sputtering from liquids. Wehner *et al* [1] bombarded liquid Sn with Ar$^+$ ions. Their results showed a 40% increase in yield compared to solid Sn at a bombardment energy of 0.2 keV and a 6% reduction at 0.4 keV. Krutenat and Panzera [2] performed similar experiments but concluded that at 0.2 keV the yield was enhanced by a factor of two and at 0.4 keV only by 15%. Cooper and Hurst [3] bombarded liquid and solid In with Ar$^+$ ions and discovered that the yield was 10% higher than the solid at 0.107 keV. Dumke *et al* [4] bombarded a Ga/In alloy whose surface monolayer is > 94% In. The measured sputtering yield ratios were found to be 28 times greater than that expected by the stochiometry which led to the conclusion that 85% of the sputtered atoms originated from the surface monolayer.

† Deceased 24 August 1988.
‡ On leave from Loughborough University, Loughborough LE11 3TU, UK.

Computer simulations of sputtering from liquids have also been carried out. Lo *et al* [5] and Shapiro *et al* [6] examined sputtering from liquid Cu with targets generated using both semi-periodic and box boundary conditions. They concluded that over 86% of sputtered atoms originate from the surface layer and that the calculated broadening in the angular distributions of sputtered atoms was due to the stochastic nature of the liquid surface. Morgan [7] has attempted to describe the nature of the liquid–vacuum interface more accurately by using a stratified model of the liquid surface with variable density. However, this is not attempted in the preliminary investigation reported here.

2. Liquid target generation

In order to generate a liquid target, an initially solid crystal was warmed by displacing the atoms from their zero degree equilibrium configuration. The initial arrangement of atoms used for all liquid simulations was a face-centred cubic (FCC) crystal consisting of 1445 atoms, whose surface was in the (111) orientation. The program used in this work for both the target generation and sputtering simulations was based on the QDYN molecular dynamics code [8, 9]. The simulations are carried out using a classical mechanics formalism and numerically solving Newton's equations of motion. The programs were run assuming that the interatomic forces are derived from pair potential interaction functions of the Born–Mayer type. The Ar^+/Cu potential function used was Shulga's modification to the standard Molière potential (modified Bohr radius $a_0 = 0.092$ Å). The Cu/Cu atom–atom potential was a repulsive Born–Mayer potential smoothly splined to a Morse well and has been previously used in studies of inert gas ion bombardment of Cu [10]. Further detailed information about these potentials may be found in [8].

In order to generate the liquid target, two methods were examined. The first method (QLV) involved assigning a velocity and random direction to each atom in the crystal. The motions of the particles were then calculated using the code with these initial conditions until equilibration between the kinetic and potential energies had taken place. The target was then tested for its liquid properties after equilibration. The magnitude of the velocity initially assigned to each atom was obtained from the product of the speed of interest $\bar{v}^2$ and a random number chosen to lie between 0 and 2 but normally distributed about unity with a standard deviation of one. The value of $\bar{v}^2$ corresponded to twice the desired value of kinetic energy in order to allow for equipartition of half the added energy into potential energy. Thus $\bar{v}^2 = 6kT/m$, where m is the mass of a Cu atom, k is Boltzmann's constant and T is the final target equilibration temperature.

The second method (QLP) warmed the target by assigning thermal displacements to all the atoms. The mean square displacement, $\bar{u}^2$, can be measured experimentally but these measurements are for temperatures well below the liquid phase and so the warming was carried out in cycles. Each atom was displaced several times before the molecular dynamics program was run, until a suitable temperature was achieved. This criterion was established by evaluating the added potential energy after each displacement cycle. Each cycle displaces atoms by an amplitude corresponding to 300 K using the same statistical distribution as in the velocity warming method. The temperature of 300 K was chosen because the corresponding thermal amplitude was a data point in the experimental results of Singh and Sharma [11]. The thermal amplitude used in the simulation was 0.0782 lattice units (LU). Here we use the convention that

two lattice units is equivalent to the FCC cell edge which for Cu is 3.615 Å, thus 0.0782 LU = 0.141 Å. When the added potential energy corresponded to twice the kinetic energy needed to produce the required target temperature, no further atomic displacements were effected.

Thermal equilibrium was achieved by running the molecular dynamics simulations until the energy became equipartitioned between kinetic and potential energies and when the Cartesian components of total kinetic energy in the target became the same. The chosen target temperature for all targets was 1462 K and equilibration always occured within 3.0×10^{-13} s (300 fs).

The simulations were run with and without boundary conditions. The boundary conditions require the atoms to experience reflection and are chosen to form a rectangular box which has been uniformly expanded from the original crystal size to correspond to the reduced density of Cu at 1462 K. The acronyms QLVBC and QLPBC refer to results from runs with the boundary conditions imposed. The simulations QLP and QLV were run without boundary conditions (i.e. free boundaries) to investigate the overall system expansion due to the interatomic interactions. It was also intended to investigate a system with periodic boundary conditions. However, all four target production methods described above produced targets with good liquid properties and so to minimise computing time, periodic boundary conditions were not investigated.

3. Liquid target simulation results

### 3.1. Target equilibration

Since the system is non-dissipative, energy is conserved and the energy conservation of the calculation provides a test of the accuracy. The simulations conserved energy with an error which ranged from 0.001% to 0.25%. The equivalent energy uncertainty summed over all 1445 particles is 0.03 eV and 6.45 eV. The mean error corresponded to a temperature of 34 K which might prove critical if simulations were carried out near the melting point. This is not the case here.

The targets with unrestricted boundaries showed the least liquid-like properties. This is to be expected since expansion had caused the target density at equilibration to be considerably less than the correct value of 7.8 g cm^{-3}. The calculated densities were respectively 6.62 for QLP and 7.66 for QLV, showing that the target with added potential energy had expanded most before equilibration. These results were the principal reason for not using the targets generated by QLP and QLV for the sputtering simulations. When the reflecting boundary conditions were applied, the density of the target was controlled, since the number of particles contained within the fixed volume defined by the boundaries remains constant. Yield statistics are dependent on target density and it is important to have the correct density in the initial target.

A plot of the components of kinetic energy against time for one of the targets is shown in figure 1. The energy rapidly becomes equipartitioned but more quickly for QLV than for QLP. All targets tested reached equilibration within 300 fs. These times are consistent with the results of Lo *et al* [5]. The simulations were computed for at least twice the calculated equilibration time in all cases.

Equipartition of energy occurred in all cases. In particular QLPBC produced a final kinetic energy, summed over all particles in the target, of 273 eV (i.e. 0.19 eV per atom), less than 1 eV different from the expected value. QLV and QLVBC gave the smallest kinetic energy oscillations at equilibrium of ± 4 eV for the whole target of 1445 atoms,
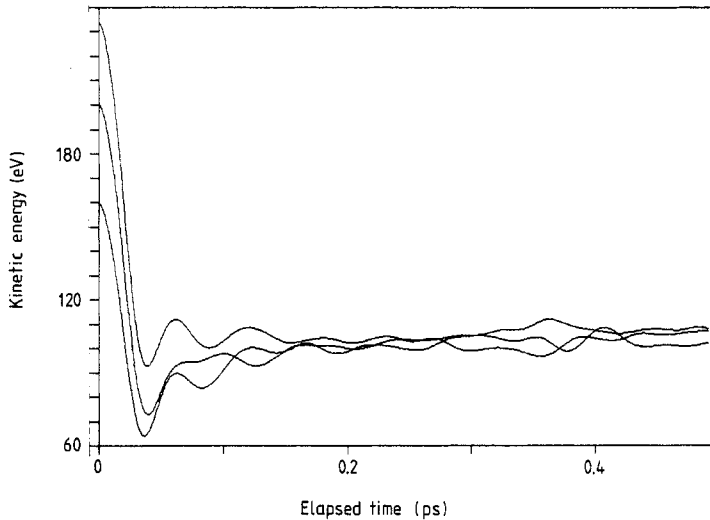
Figure 1. The components of kinetic energy as a function of elapsed time for QLVBC. The components refer to the total sum over all 1445 particles of the target. The oscillations in these components persist for slightly longer than the time for which equipartition between kinetic and potential energy occurs.

corresponding to a temperature of 48 K. This would be expected to diminish if the number of atoms in the system were to be increased.
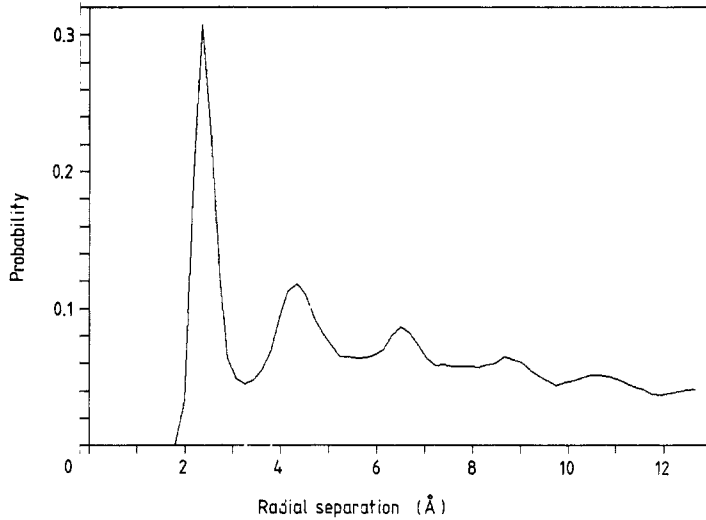
3.2. Radial distributions

The liquid state has a very distinct radial density distribution $G(r)$, and before carrying out simulations of keV particle bombardment on a liquid target it was thought necessary to test the calculated radial distributions against those reported in experimental measurements. The radial distribution plotted in figure 2 is the function

$$G(r) = 4\pi r^2 \rho(r)$$

where $\rho(r)$ is the density of atoms at a distance r away from a given atom. The peaks and valleys of the calculated distribution function are compared in table 1. The best agreement with experiment is from the simulation QLVBC. The radial distribution was calculated for the most central atom in the target in order to minimise edge effects. The distribution shown in figure 2 has the distinctive wide and smooth peaks and valleys characteristic of a liquid and is in excellent agreement with experimental neutron diffraction data [12].

3.3. Velocity distributions

The calculated velocity distributions after target equilibration were compared to the Maxwell–Boltzmann distribution. The results show that all the distributions calculated for all the targets generally match the Maxwellian distribution. The reduced χ^2 tests and their probabilities $P_d(\chi^2 \geq \chi_o^2)$ are shown in table 2. This shows that only QLVBC has a velocity distribution with $P_d(\chi^2 \geq \chi_o^2) > 5\%$, the standard rejection criterion. The smallest $P_d(\chi^2 \geq \chi_o^2)$ was 0.5%. The statistics would be improved by choosing a larger number of particles N_t in the system. However, the χ^2 test shows that the chosen number of $N_t = 1445$ gives reasonable statistics and this number also does not require excessive use of computer time.

Figure 2. The radial distribution function for the most central atom within the target for QLVBC.

Table 1. A comparison between the peaks and valleys of the radial distributions compared to experimental data taken from [12]. Distances are in LU.

| Target	1st peak	1st valley	2nd peak	2nd valley	3rd peak	3rd valley
QLP	2.4 ± 0.1	3.3 ± 0.1	4.3 ± 0.1	—	6.6 ± 0.1	—
QLPBC	2.4 ± 0.1	—	4.4 ± 0.1	—	6.6 ± 0.1	—
QLV	2.4 ± 0.1	3.3 ± 0.1	4.3 ± 0.1	—	6.6 ± 0.1	7.7 ± 0.1
QLVBC	2.4 ± 0.1	3.3 ± 0.1	4.3 ± 0.1	5.6 ± 0.1	6.5 ± 0.1	7.7 ± 0.1
Experimental data	2.5 ± 0.1	3.5 ± 0.1	4.7 ± 0.1	5.6 ± 0.1	6.8 ± 0.1	7.9 ± 0.1

Table 2. The χ^2 test data for the goodness of fit of the computed velocity distributions with the Maxwell–Boltzmann distribution.

Target	χ^2	$P_d(\chi^2 \geq \chi_0^2)$
QLP	1.7	1.6
QLPBC	1.9	0.5
QLV	1.5	5.4
QLVBC	1.5	1.5

4. Sputtering simulations

The sputtering simulations were carried out separately from the target generation process using the same pairwise interaction potentials described in §2. A detailed description of the calculations for ejection of material from solids under keV particle bombardment pair potentials is given in [8]. Pair potentials overestimate the experimentally measured sputtering yields and more accurate energy and angular distributions can be obtained by using many-body interaction potentials, such as the embedded atom method [13], if required. Electronic energy loss was not taken into account in the model. For the liquid bombardment, a single target was used throughout and

the impact point varied over the surface in order to obtain a statistical distribution of yields. To obtain even better statistics, the target itself should also be regenerated before each run. However, tests [14] have shown that a change of target has only a minimal effect on the sputtering statistics if the atoms within the target are arranged in a sufficiently random manner. The yields and angular distributions are not distorted by retaining the same initial atom positions, the maximum deviation of calculated yields being 3.5%. The target obtained from QLVBC was chosen for the sputtering simulation because it has the best overall liquid-like characteristics. The initial positions of the atoms in this target are shown in figure 3. For a regular crystal lattice, there is a small area on the surface of the crystal over which a set of impact points can be distributed to give a sample that is representative of the crystal as a whole [8]. For a liquid, the lack of structure means that no such easily identifiable area exists. The simulations here were carried out with a set of 300 impact points at normal incidence, distributed over an area 3.6 Å × 3.6 Å, which is equivalent to the unit cell on the (010) surface. Two other trajectory sets were also calculated corresponding to a target with a low-index Cu surface (010) with 1626 atoms and a target with a high-index surface (3 11 1) consisting of 1616 atoms. A high-index plane was chosen for comparison because the surface atoms are less tightly bound (calculated surface binding energy 1.74 eV for the (3 11 1) face) than for the (100) orientation (2.43 eV) and the crystal structure appears more random when viewed from the perspective of the incoming particle. The reason for the choice of the (3 11 1) crystal orientation was because strange surface topography has been observed to develop after high doses of inert gas ion bombardment and a set of data had been generated as part of a more detailed study of keV particle bombardment of this face [15].
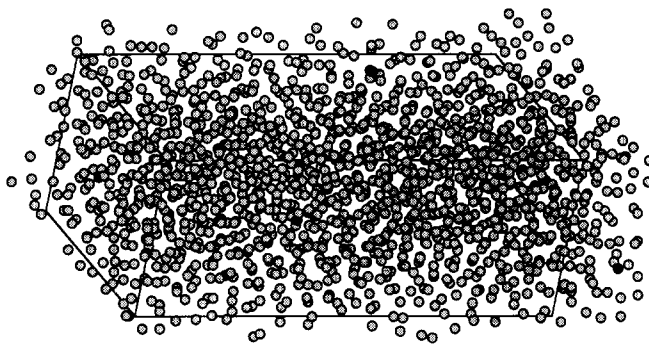
Figure 3. A perspective view showing the initial atom positions in the chosen sputtering target. The outlined box defines the boundaries of the initial crystal before expansion. Atoms with energy > 0.5 eV are shown darker.

The sputtering calculations were carried out differently from simulations used in the target generation. From experience gained over a number of years, it has been found best [8] to use free boundaries for sputtering calculations. This is because the collision cascade propagates like a tree as the incoming particle loses its energy to the surrounding atoms. If the target is sufficiently large, most of the hard collisions will have occurred by the time the cascade propagates to the sides of the target. Channelled higher-energy particles can also leave the bottom of the target but these have no effect on the yield statistics. The cascade propagates much faster than any thermal motion

(see §5) and any effects near the boundaries due to thermal motions are small and do not affect the yield statistics. Thus particles that leave the sides or bottom of the target during the sputtering calculation are simply ignored.

5. Sputtering results

The calculated yield is shown in table 3 along with a comparison of calculated and measured yields for both crystalline and polycrystalline Cu. No experimental results for liquid Cu appear to be available.

Table 3. Calculated and experimentally measured yields for 1 keV Ar^+ bombardment for Cu at normal incidence. The experimental results are for polycrystalline Cu collated from a series of experiments [16].

Cu(100)	Cu(3 11 1)	Liquid Cu	Experiment
6.2	5.9	8.4	2.0–4.0

The pair potential formulation is known to overestimate the measured sputtering yields and therefore the results for the liquid should be seen as a comparison with the solid data, rather than an absolute determination of the yields. It is possible to obtain closer agreement with experiment by a different choice of interaction potential but since the experimental measurements are performed for amorphous Cu which also contains implanted Ar, a direct comparison between the simulations and the experiments is never an accurate comparison. The final average yield for the liquid target is 8.4 atoms per ion which is 36% higher than that calculated for the (010) face. Such a large result was unexpected because the average kinetic energy per atom due to thermal effects is of the order of 0.1 eV, whereas the bulk crystal binding energy is 7.0 eV. However, the density of the liquid target near the surface turned out to be somewhat less than in the bulk. It appears that this is a critical factor in assessing yields and its effect would need to be studied further in any future work on the sputtering from liquids. An increase in the yield of ejected particles was to be expected from the calculations. The density of the bulk liquid target is less than the bulk solid and the more random distribution of material within the target means that there are more open spaces near the crystal surface which allows energetic material to escape. There are also a number of near-surface atoms that are less tightly bound to the bulk than for the solid targets. The precise values of the calculated yields can be improved by using a larger sample data set. The statistical accuracy of the calculated yields should be within 5% using our uniform sampling technique with 300 impact points but the energy distributions often need a much larger set. As many as 5400 [17] have been found to be necessary to model accurately the energy distributions and the computing time required to calculate these is immense. There are also errors inherent in the numerical integration algorithm but these are generally small. The major sources of error are the sampling technique for the impact points and errors due to taking the same configuration of atoms to model the liquid state discussed in §4. The calculations for the yields from the liquid state should therefore be accurate to within about 8.5% and those for the solid to within 5% .

Figure 4 shows a comparison between the liquid and solid data. The spot pattern (azimuthal angular distributions of ejected material) for the liquid is radially symmetric
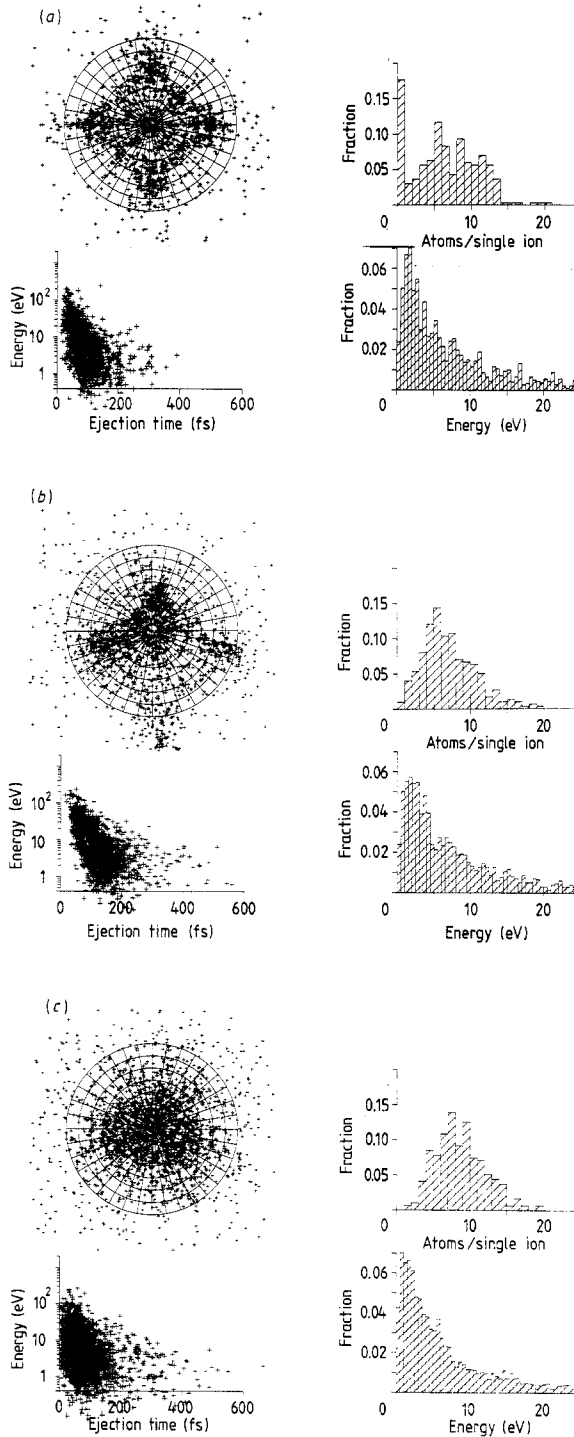
Figure 4. Multiple plots of sputtering data from the solid and liquid crystal targets. (*a*), (010) plane; (*b*), (3 11 1) plane; (*c*) the liquid target. The plots show the spot patterns, the yield and energy distributions and the energy of emitted particles at the time they were emitted, as a function of that time.

and shows no sign of crystal lattice effects. The azimuthal angular distribution for the liquid shows much more wide-angled scattering than for the solid crystal targets due to the lack of a well defined interface as in the case of a solid crystal. The yield distribution (atoms per single ion) is regularly distributed about the mean. In contrast, a number of trajectories for the (010) face have zero yield due to channelling. The energy distribution for the liquid shows a higher peak at lower energies than for the solid crystal targets. However these are known to be inaccurately predicted by pair potentials with the peaks being at energies that are lower than those experimentally observed. The other distinguishing feature of the liquid and high-index crystal planes are the longer ejection times of atoms from some trajectories. These times are still well below timescales characteristic of thermal processes. During a typical cascade in which all atoms are ejected within 500 fs, a typical liquid atom, which is not involved in a collision and whose average velocity is 800 m s^{-1}, would travel a distance of about 4 Å. Since most atoms are ejected before 500 fs, the target is almost 'frozen' during the cascade. It is therefore expected that results from the liquid target should also be representative of those from an amorphous solid. A few results have also been obtained using the embedded atom potential for Rh under 1 keV Ar$^+$ ion bombardment [14]. These results indicate a similar trend in the atoms per single ion distributions but a much lower yield increase for the liquid compared to the solid, close to 10% instead of 40%. In addition they show less comparative angular spread than for the case of pair potentials. The embedded atom method has the computational advantage of a pair potential formalism but uses a many-body description of the atomic interaction forces which do not scale linearly with the presence of neighbours. This allows a more accurate model of the forces which occur near surfaces. The combination of the embedded atom formalism together with a more accurate description of the surface should enable improved molecular dynamic calculations of sputtering from liquid metals.

Acknowledgments

References

[1] Wehner G K, Stewart R V and Rosenberg D 1962 *General Mills Report No* 2356
[2] Krutenat R C and Panzera C 1970 *J. Appl. Phys.* **41** 12
[3] Hurst B L and Cooper C B 1982 *J. Appl. Phys.* **53** 9
[4] Dumke M F, Tombrello T A, Weller R A, Housley R M and Cirlin E H 1983 *Surf. Sci.* **124** 407
[5] Lo D Y, Tombrello T A and Shapiro M H 1986 *Nucl. Instrum. Methods* B **17** 207
[6] Shapiro M H, Lo D Y, Haff P K and Tombrello T A 1986 *Nucl. Instrum. Methods* B **13** 348
[7] Morgan W L 1989 *J. Appl. Phys.* **65** 1265
[8] Harrison D E 1988 *Crit. Rev. Solid State Mater. Sci.* **14** S1
[9] Harrison D E 1983 *Radiat. Eff.* **70** 1
[10] Webb R P and Harrison D E 1983 *Phys. Rev. Lett.* **50** 1478
[11] Singh N and Sharma P K 1971 *Phys. Rev.* B **3** 4
[12] Eder O J, Erdpresser E, Kunsch B, Stiller H and Suda M 1980 *J. Phys. F: Metal Phys.* **10** 183

[13]   Garrison B J, Reimann C T, Winograd N and Harrison D E 1987 *Phys. Rev.* B **36** 3516

[14]   Fisher M L 1988 *MS Thesis* NPS, Monterey

[15]   Smith R and Harrison D E 1989 *Phys. Rev.* B **40** at press

[16]   Anderson H H and Bay H L 1981 *Sputtering by Particle Bombardment* ed. R Behrisch (Berlin: Springer) ch 4, pp 176–7

[17]   Smith R, Harrison D E and Garrison B J 1989 *Phys. Rev.* B **40** 93